



ISSN NO. 2320-5407

Journal Homepage: -[www.journalijar.com](http://www.journalijar.com)

## INTERNATIONAL JOURNAL OF ADVANCED RESEARCH (IJAR)

Article DOI:10.21474/IJAR01/7955  
DOI URL: <http://dx.doi.org/10.21474/IJAR01/7955>



### RESEARCH ARTICLE

#### THERMO-MECHANICAL PROPERTIES OF HIGH-PERFORMANCE NATURAL POZZOLAN CONCRETE.

**Eddie Franck Rajaonarison<sup>1</sup>, Bam HajaNirina Razafindrabe<sup>2</sup> and Lalaina Dina Prisca Rajaonarison<sup>3</sup>.**

1. Materials Science and Metallurgy, EcoleSupérieurePolytechnique, University of Antananarivo, 101 Antananarivo, Madagascar.
2. Faculty of Agriculture, Ryukyu University, 1 Senbaru, Nishihara, Okinawa 903-0213, Japan.
3. INGE, Planning and Territory, University of Antananarivo, 101 Antananarivo, Madagascar.

#### *Manuscript Info*

##### *Manuscript History*

Received: 17 August 2018

Final Accepted: 19 September 2018

Published: October 2018

##### *Keywords:-*

Superplasticizer, natural pozzolan, high performance concrete, mechanical strength, Conductivity and thermal diffusivity.

#### *Abstract*

Researches and obtainable results on natural pozzolan particles, to make lightweight concretes, are proven to be very rare. This work has been conducted in the thermo-mechanical properties of the natural pozzolans in lightweight concrete. The use of lightweight concrete has allowed us to expand the field of use of concrete. The goal of this work is to achieve a high-performance lightweight concrete at a competitive cost and minimal environmental impact with natural pozzolans.

*Copy Right, IJAR, 2018,. All rights reserved.*

#### **Introduction:-**

The essential novelty that appeared in concrete technology in the 1980s is the increasing use of superplasticizer additives [1]. These products have the ability to turn a firm consistency concrete into a fluid suspension, which spreads and fills a container under its own weight [2]. They can also be used to reduce the amount of mixing water in a proportion of the order of 30% while keeping the mixture maneuverability allowing its implementation by the usual methods [3]. Madagascar is one of the developing countries, it adapts the sustainable development program in all areas especially in the field of construction industry, so it is necessary to manufacture sustainable concrete. Recent developments in cement and cement additive technology (silica fume, natural pozzolan) and superplasticizers have led to the production of lightweight, high-strength concrete [4], its high resistance is an inverse function of its total vacuum content.

This work is part of the implementation of natural mineral resources Malagasy. It aims to minimize the cost of construction through the use of proper technique and materials. More specifically, this work studies natural pozzolana aggregates from the Ambohinaorina\_Madagascar. The current trend in the individual building, is to favor light products able to fulfill several uses.

As the porosity increases, the mechanical strength of a concrete decreases [5]. This phenomenon has been confirmed by JBu and Z Tian [6] on the compressive strength of light concretes, which is a decreasing function of the volume fraction of aggregates.

The second originality of this work concerns the specific characteristics of natural pozzolana concrete. This specificity is due to the properties of each constituent as well as the resulting microstructure of the mixture thereof. In this context, the exploitation of the experimental results facilitates the definition of the reformulation of pozzolan concretes.

**Corresponding Author:-Eddie Franck Rajaonarison.**

Address:- Materials Science and Metallurgy, EcoleSupérieurePolytechnique, University of Antananarivo, 101 Antananarivo, Madagascar.

**Materials:-****Cement:-**

The cement used is the type I (ASTM C 150) [7]. The physical properties and chemical composition are listed in Table 1.

**Table 1:-**Chemical compounds and physical properties of cement.

Chemical compounds	%	Physical properties	%
SiO <sub>2</sub>	21.01	Specific gravity (g/cm <sup>3</sup> )	3.12
Al <sub>2</sub> O <sub>3</sub>	5.39	Specific surface (Blaine) (cm <sup>2</sup> /g)	3350
Fe <sub>2</sub> O <sub>3</sub>	3.23	2 days compressive strength (MPa)	21.0
CaO	62.11	7 days compressive strength (MPa)	28.0
MgO	1.98	28 days compressive strength (MPa)	42.0
Na <sub>2</sub> O	0.21	Initial setting time (min)	157
K <sub>2</sub> O	0.74	Final setting time (min)	235
SO <sub>3</sub>	3.1	Soundness (mm)	1.0

**Water:-**

ASTM C1602 [8] includes provisions for drinking water and is used for mixing and curing concrete specimens .

**Pozzolan:-**

The natural pozzolana used to prepare the specimens originates from the site of Ambohinaorina, district of Betafo, Antsirabe. Its main mass, which has not been estimated, is formed by projection products, among which slags largely dominate. Pozzolan samples were subjected to the identification and characterization tests. Chemical analyses of pozzolan powder samples were conducted. The X-ray powder diffraction method was performed on the samples using a monochromatic X-ray beam. A Siemens D500 diffractometer operating with a monochromatic CuK $\alpha$  radiation at a wavelength  $k = 1.7903 \text{ \AA}$ , a voltage of 40 kV and a current of 30 mA was used. The results obtained are shown in fig. 1.

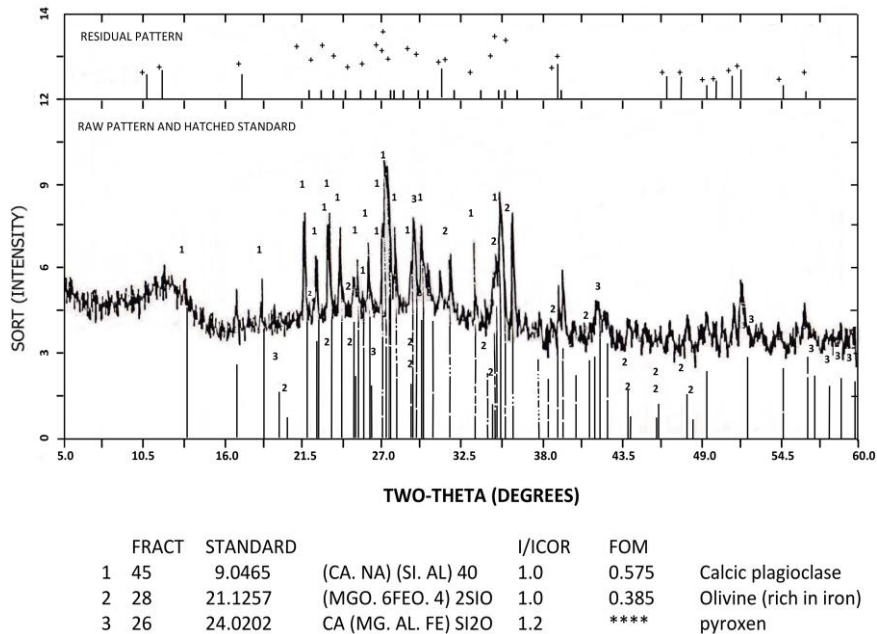
**Fig. 1:-**X-ray diffraction analysis.

Table 2 summarizes the main characteristics of the scoria samples used for this study while Table 3 shows the results of the chemical analyses for these samples.

**Table 2:-**The samples from the considered quarry

Color	Form	State of surface	Structure	Appellation
purplish-blue black	scoriaceous	Very rough	Porous	scorias

**Table 3:-**Chemical analysis of pozzolan.

Elements	%
SiO <sub>2</sub>	48,70
Al <sub>2</sub> O <sub>3</sub>	20,12
Fe <sub>2</sub> O <sub>3</sub>	01,13
CaO	10,58
MgO	09,81
K <sub>2</sub> O	01,10
SO <sub>3</sub>	00,00
TiO <sub>2</sub>	02,81
MnO	00,22
Na <sub>2</sub> O	02,78
Cr <sub>2</sub> O <sub>3</sub>	00,10
P <sub>2</sub> O <sub>5</sub>	00,64
LOI	02,00
TOTAL	99,99

Note that we have followed ASTM C618 [9] standard which intend to set pozzolan characteristics. Pozzolan is a natural rock, generally black or red, made of volcanic scorias; the pozzolan silica, alumina, and ferric oxide average value has to be between the following limits: SiO<sub>2</sub> from 43 up to 55%, Al<sub>2</sub>O<sub>3</sub> from 12 up to 24%; Fe<sub>2</sub>O<sub>3</sub> from 8 up to 20%. Those limits intend particularly to ensure cohesion between chemical elements.

The fines used for some of the mixtures were 100µm constituents taken from the pozzolans grinding.

#### **Sand:-**

The influence of the sand on the resistance of mortars will be investigated. Their physico-chemical characteristics are set out in Table 4.

**Table 4:-**Physicochemical characteristics of sands

Elements	Physico-chemical
Mineralogical composition	Limestone
Origin of sands	Rolled with rounded grains
Particle size distribution	Rolled 0/4 mm
Los Angeles Trial	33
Micro-Deval wear test	20
% Water absorption rate	04.10

#### **Superplasticizer:-**

The adjuvant used is a water-reducing plasticizer for high-performance concretes in accordance with the NF EN 934-2 standard [10]. The SIKAMENT FF 86 allows the manufacture of concretes with very low E / C ratio having very high mechanical strengths at all times and especially at young ages.

#### **Method:-**

From the theoretical and experimental point of view, a number of authors have carried out work on the behavior of granular mixtures in order to obtain an optimal formulation of concretes [11]. The latter is nevertheless acknowledged to be unreachable because the various parameters to be considered in the study, according to DREUX [12] are extremely numerous.

The research process has led to some rules for usefully channeling the practice of concrete composition.

With regard to common concretes, the main objective has always been to produce and obtain concretes with minimal porosity which, by the logical rule, offer the best mechanical resistance on a sustainable time scale.

The goal for lightweight aggregate concrete which is slightly different from conventional concrete is to obtain rules of mixtures compatible with the composition of concretes commonly having acceptable mechanical strengths, a low density and good physical characteristics [13].

Thus, it is important to extend the theory of mixtures of two ordinary aggregates for the case of porous aggregates. Added to this is the experimental study of the existing problem.

We will take into account two different aggregates between them by their grain size. We will call conventionally one of them, the coarse aggregate and the other the fine aggregate, if one refers to the comparison of their respective dimensions.

If it is assumed that the fine aggregate has a size  $d$ , an apparent volume  $V_{ap}$  and an absolute volume  $V_{ab}$ , its expansion  $f$  is equal to  $V_{ap} / V_{ab}$ .

Weight by weight, if a few grains are replaced by a single large grain of volume  $v$ , the apparent volume of the granulate increases by  $v(f - 1)$ .

Taking into account the wall effect of fine grains on coarse grains, moreover, if  $V$  is the volume gained per unit area of a coarse grain and at its surface, the total volume gained is  $nAV$ .

At each substitution, an apparent volume increase is obtained which is expressed by:

$$\Delta V_{ap} = v(f - 1) + nAV \quad (1)$$

If we start from the choice of unit volume of matter and let  $\sqrt{v}$  the volume of fine grains remaining after  $n$  substitutions, their apparent volume is  $\sqrt{v}f$ .

By hypothesis, in this volume which is reduced, the fine aggregate retains the same structure and the same index of voids out of the immediate vicinity of the coarse grains.

The volume of coarse grains is expressed by  $(1 - \sqrt{v})$  and the surface effect leads to an increase in  $nAV$ . Thus we obtain a total apparent volume of:

$$V_{ap} = \sqrt{v}(f - 1) + nAV + 1 \quad (2)$$

However,  $A = cv/d$  where  $c$  is the coefficient of proportionality between the volume of large grains and that of fine grains. If we put  $c/d = C$ , then  $V_{ap} = \sqrt{v}/(f - 1) + CnvV + 1$  with:  $nv$  coarse volume:  $nv = (1 - \sqrt{v})$

$$V_{ap} = \sqrt{v}(f - 1 - CV) + CV + 1 \quad (3)$$

If we assume that:  $\gamma$  = density of the material, the weight of the fine grains in the mixture is given by the relation:  $P = v/\gamma$

$$\text{so} \quad V_{ap} = (P/\gamma)(f - 1 - CV) + CV + 1 \quad (4),$$

it is an expression of the form:  $V_{ap} = XP + \text{const}$  because  $C$ ,  $\gamma$ ,  $f$  and  $V$  prove constant. Since  $e$  represents the void index of the mixture, as follows:

$$V_{ap} = V_{\text{vide}} + V_{\text{material}} = e + 1$$

Hence the relation (3) becomes:

$$e = \sqrt{v}(f - 1 - CV) + CV \quad (5)$$

$$e = (P/\gamma)(f - 1 - CV) + CV \quad (6)$$

It can be seen that the value of  $f$  is close to 2. Therefore, the substitution of the large granulate for the fine granulate tends to decrease the apparent volume corresponding to the void ratio of the mixture studied.

If one starts from a large aggregate and if one supposes that one could replace it in part and by weight by weight for a fine aggregate and, in addition if  $f'$  present the expansion of the big aggregates, thus the apparent volume during which the fine grains associate with the fat is expressed by the relation:

$$V_{ap} = f' v_r$$

where  $v_r$  = volume of the rest of the coarse grains

Hypothesis: « it is assumed that the structure of the coarse aggregate remains unchanged »

With:  $1 - v_r$  = volume of fines in substitution,  
the empty index is expressed by:

$$e = f' v_r - 1 \quad (7)$$

We obtain as follows:  $V_{ap} = \left( \frac{f'}{\gamma} \right) e$  et

$$e = \left( \frac{f' P}{\gamma} \right) - 1 \quad (8)$$

The combination of relations (5) and (7) leads to the existence of a binary mixture where the apparent volume (the void ratio) is maximal. In theory, this volume must be at the intersection of the two lines formed by the relations (6) and (8).

Another type of interaction is experimentally encountered in this study other than the wall effect. This is the granular interference effect [65] in coarse aggregates in the mixture. This threshold disrupts them at the granular level, leading to the increase of the void index with respect to the theoretical index.

#### Case of two porous aggregates:-

The void ratio expressed in relation (7) can be expressed by:

$$e = (f' - 1) v_r - (1 - v_r)$$

As all the aggregates are porous, so:

$$e = f' (1 + E) v_r - 1 - E \quad (9)$$

hence:  $V_{ap} = f' (1 + E) v_r - E$

It can be seen that the line described by relation (9) is more or less in the form of an increase in slope by means of the relation (7). The index of grain voids also influences the constant term.

#### When only the large granulate is porous:-

The addition of coarse aggregate and non-porous fines does not affect the modification of equation (7). It remains

$$e = f' (1 + E) v_r - 1$$

So,

$$V_{ap} = f' (1 + E) v_r$$

The same slope is relative to the relation (9). In conjunction with the weight:  $V_{ap} = f' (1 + E) \left( \frac{P}{\gamma} \right)$

As a conclusion, by interchanging large granules and fine granules, we have a relation:

$$e = \alpha V_{ab} + \beta \quad (10)$$

Where,  $\alpha$  and  $\beta$  are the void ratio coefficients and grain forms, and  $V_{ab}$  is aggregate absolute volume in concrete  $\text{Im}^3$ .

#### Cement compatibility / superplasticizer:-

Slump loss, setback, stiffening, or disruption of the entrained air content are all synonymous with cement / superplasticizer incompatibility [14]. The study of cement / superplasticizer compatibility (C / SP) is done by the flow test of Marsh cone types. The method used is to prepare a slurry and measure its flow time at 5 and 60 minutes.

The C / SP combination studied is compatible and the saturation point is very high (4.2%) because the solids content of the superplasticizer used is more or less low of about 20%.

#### Concrete composition:-

We noticed that the grain forms have an influence on the void ratio corroborated with the plate effects and the aggregate interference. So, an experimental study is imperative for a better understanding of the interaction between fines and big aggregates. This behavior can be observed on a scoriaceous form such as natural pozzolans. For ternary mixtures: the sand, fine and gravel interaction has to be analyzed. On the one hand, concerning sands, fines

and gravels, they confirm their behavior as binary mixtures. Ternary mixtures require an experimental study to understand the influence of the void ratio variations.

For binary mixtures, the pozzolans aggregates real volume ( $V_r$ ) is constant for the compositions categorized by specimen from bc1 to bc6. We reduced progressively the cement dosage to respect void ratio results. The fines quantities used have been calculated to respect the mixture absolute volume total value (in cement substitution).

It is worth noting that for bc7 and bc8 specimens, we reduced the  $V_r$  quantity to make its effectiveness significant on the void ratio. Table 5 gives the mixture compositions made in this study.

**Table 5:-Binary concretes composition**

Denomination	bc1	bc2	bc3	bc4	bc5	bc6	bc7	bc8
Vc	145	141	123	121	116	86	133	121
Vf	183	221	140	78	00	00	253	286
Vab	299	299	299	299	299	299	244	187
Vr	538	538	538	538	538	538	432	334
water	141	141	141	141	141	141	141	141
superplasticizer	31	31	31	31	31	31	31	31

Where: Vc is volume of cement, Vf is volume of fines, Vab is absolute volume of aggregates in 1m<sup>3</sup> of concrete, and Vr is real volume of the pozzolan aggregates.

For ternary mixtures, the experimental volumetric method is determined according to the ASTM C33 [15] norm. For this latter, concerning solid constituent dosages, big aggregates are considered on their real volume after pre-soaking. These aggregates are pozzolan pea gravels including to 5/10 series. The sand used was an ordinary one. The various concrete compositions are listed in table 6.

**Table 6:-Volume of the constituents of the ternary concretes in litre for 1 m<sup>3</sup>.**

Name	A				B					C				
	1	2	3	4	1	2	3	4	5	1	2	3	4	5
Specimens n°														
Dosage (Kg/m <sup>3</sup> )	250	350	350	300	450	425	400	350	450	450	450	450	450	350
Sand	68	105	162	231	72	191	252	292	332	71	139	237	291	361
Cement	82	115	124	92	147	132	132	116	115	137	136	123	114	111
Fines	00	00	00	00	50	34	13	00	00	156	136	98	110	47
Water	100	133	133	100	146	146	142	126	133	180	184	156	113	156
Pea gravel	538	538	538	492	538	470	385	358	301	464	402	333	230	260
superplasticizer	22	30	30	22	32	32	32	28	30	40	41	35	25	35

For each series, we added progressively and quantitatively sand.

For series A, fines were not used and the pea gravels quantity was the same for specimens n°1, 2 and 3. During the operations, the sand quantity and cement dosage were increased. For specimen n°4, we reduced the pea gravel amounts in increasing the sand amount compared to the previous ones. The cement dosage is listed in table 8.

For series B, we did not use the fine for specimens n°4 and 5. In these batches, the sand amount used was increased and the pea gravel, fine and cement amounts were progressively reduced. You can obtain these results from a binary concrete belonging to "semi- cavernous" series.

For series C, we made a cement dosage fixed to 450Kg/m<sup>3</sup>, for specimens from n°1 to n°4, by increasing progressively the sand amount. On the other hand, the cement dosage was reduced to 350Kg/m<sup>3</sup> for batch n°5. Its special detail is the fine sequential reductions.

The aggregate amount calculations used will help us to define the mixtures according to the concrete that we want to make, either a fat or no-fine one.

The formulations choice is made according to the elements we want to analyze: the aggregate quality influences, volumetric concentration and on natural lightweight pozzolan concrete mechanical, thermal and acoustical behavior.

### Mechanical properties:-

Concretes mechanical characteristics are usually more analyzed, and, better known because of the very important structural role played by concretes in civil engineering works.

For a lightweight concrete, the apparent density is considered to be one of the material essential properties. In this study, the apparent density is determined by finding the mass with a precision weighting balance (Perrier, French), 4\*4\*16 cm parallelepiped sample hardened.

The concretes mechanical properties are given at 28 d. The measurements were performed following ASTM C39 [16], Standards Test Method for Compressive Strength of Cylinder Concrete Specimens.

### Thermophysical properties:-

The samples subjected to these tests have a parallelepiped shape with a 27 cm side and a thickness that varies from 2 to 7 cm.

If one considers a steady state, where the flow of heat is supposed to be non-directional and crossing a homogeneous wall of thickness  $e$  under uniform temperatures  $T_1$  and  $T_2$  on both sides.

The equation of the heat flux  $\phi$  that passes through the face  $A$  of the sample, is expressed by:

$$\phi = (\lambda/e) (T_2 - T_1) A \quad (11)$$

We can deduce the thermal conductivity by the following relation:

$$\lambda = \phi e / (T_2 - T_1) A \quad (12)$$

In practice, the heat exchanges between the box and the outside are not always null.

This is because of the difficulty of uniformly obtaining a temperature  $T_B$  inside the box equal to that outside  $T_A$ .

Thus, a certain loss is recorded  $\phi_0$  such that the flow becomes:

$$\Phi_T = \phi + \phi_0 \text{ et } \phi_0 = C' / (T_A - T_B) \quad (13)$$

Where  $C'$  is the coefficient of loss of the box

The theoretical value of the coefficient of loss  $C'$  is ordinarily determined by the formulas of Carslaw and Jeager on one side, and by that of Langmuir on the other side. This being because of the parallelepipedal shape of the box. The first expressions describe the flow of heat through a dihedron in steady state, the second establishes the value of the form factor for the corners of a cube.

According to the characteristics of the box, we obtain the following relation:

$$C' = \frac{4\lambda' ab}{d} + \frac{\lambda'' a^2}{d'} + \frac{8b\lambda' (\text{Log } 1/2 + 2\text{Arctg } 1)}{\pi} + \frac{8a\lambda'' (\text{Log } 5/8 + 1/\text{Arctg } 2 + 2\text{Arctg } 1/2)}{\pi} + \frac{0,6d^2}{a^2} \quad (14)$$

with:

$$\frac{\lambda'}{d} = \frac{1}{(d_1 / \lambda_2 + d_2 / \lambda_2)}$$

where :

1. a: side of the square base of hot box B
2. b: lower height of a box B
3. d1: thickness of styrodur of a vertical wall of B
4. d2: thickness of plywood surrounding the box
5. d = d1 + d2 et d' = 2 d1 + d2
6.  $\lambda_1$  : thermal conductivity of styrodur
7.  $\lambda_2$ : thermal conductivity of plywood

The value of  $C'$  is obtained experimentally by means of two different measurements of the conductivity of the temperature on a given sample. At the heating level, two voltages  $U_1$  and  $U_2$  can be applied while noting the two corresponding temperature differences  $(T_a - T_B)_1$  and  $(T_a - T_B)_2$ .

$$\frac{1}{(T_2 - T_1)_1 [U_1^2 / R + C' (T_a - T_B)_1]} = \frac{1}{(T_2 - T_1)_2 [U_2^2 / R + C' (T_a - T_B)_2]} \tag{15}$$

**Thermal Conductivity:-**

To measure the thermophysical characteristics, our samples were dried in an oven at a temperature of 50 ° C. An unidirectional heat flow passed through the samples (E) which were placed between the cold and constant isothermal heat flux sources. The thermal gradient that evolved between these two faces was measured. Once the stationary state is established, the apparent thermal conductivity [17] can be expressed by the formula:

$$\lambda a = \frac{e}{S(Tc - Tf)} \left[ \frac{V^2}{R} - C_1(Tb - Ta) \right] \tag{16}$$

where:

- $\lambda a$ : apparent thermal conductivity;
- V: voltage applied to the terminals of the heating plate;
- R: plate resistance;
- C1: coefficient of heat loss;
- Ta: ambient temperature of the experiment room;
- Tb: temperature inside the box;
- Tc: temperature of the hot face of the sample;
- Tf: temperature of the cold side of the sample;
- S: surface of the sample;
- e: thickness of the sample.

For temperature readings to calculate the thermal conductivity, it is essential that the steady state is reached. In our experiments, this was achieved six hours after the beginning of the test. The device used to measure the thermal diffusivity is the same as that of the box method for the measurement of thermal conductivity. The sample is placed in a box with reflective faces and thermally well insulated. It receives a thermal pulse from a source of constant flux radiation consisting of a 500W incandescent lamp.

**Thermal diffusivity :-**

The analytical model is based as follows:

1. One of the flat faces of the sample receives radiation from the uniform temperature for a time  $t_0$ . The absorbed energy density  $q$  is assumed constant over the duration of the temperature signal;
2. Transfers are assumed to be unidirectional. This hypothesis is verified practically by:  $r_0 / e > 5$  where  $r_0$  is the radius of the irradiated surface.
3. The thermophysical quantities are independent of the temperature This gives a linear model of analysis which in the experiment is carried out if the thermal differences are limited to a few degrees.
4. The surface exchanges on the plane faces are identical.

The equation taking into account the previous hypotheses under transient conditions is expressed by:

$$\frac{\partial^2 T}{\partial^2 x} = \frac{1}{a} \frac{\partial T}{\partial t} \tag{17}$$

The initial and boundary conditions are written as follows:

We pose for  $0 < x < e$

$$T(x,0) = 0 \tag{2}$$

and

$$q - hT(0,t) = -\lambda [\partial T / \partial x (0,t)]$$

$$h - T(e,t) = -\lambda [\partial T / \partial x (e,t)]$$

$$\tag{18}$$

The equation system is solved as a result of the function change of type:

$$T(x,t) = a_0 + a_1 t + b_1 x + a_2 t^2 + b_2 x^2 + c_2 x t + T'(x,t) \tag{19}$$

Boundary conditions of the third homogeneous type are obtained by judicious choice of the coefficients  $a_i$ ,  $b_i$  and  $c_i$ . The variable separation makes it possible to obtain the resolution itself.

During the excitation, one can obtain the following expression:

$$T(x,t) = \frac{2qe}{\lambda} \sum_{k+1} \frac{[\cos U_k (\frac{x}{e}) + \frac{p}{U_k \sin U_k (\frac{x}{e})}]}{(U_k^2 + p^2 + 2p)} (1 - e^{-\frac{aU_k^2 t}{e^2}}) \tag{20}$$

where  $p = he/\lambda$

The values of  $U_k$  are the solutions of the following equation:

$$T_{gu} = \frac{2pU}{(U^2 - p^2)}$$

Après le signal l'expressions'écrits on prend pour température  $T_1(x, t')$  :

After the signal the expression is written if we take for temperature  $T_1(x, t')$  :

$$\frac{\partial^2 T_1}{\partial^2 x} = \frac{1}{a} \frac{\partial T_1}{\partial t} \tag{21}$$

With the solutions:

$$\left. \begin{aligned} 1. \quad hT_1(0,t') &= \lambda \frac{\partial T_1}{\partial x}(0, t') \\ 2. \quad hT_1(e,t') &= -\lambda \frac{\partial T_1}{\partial x}(e, t') \\ 3. \quad T_1(x,0) &= T(x,t_0) \end{aligned} \right\} \tag{22}$$

Where  $t_0$  is the warm-up time

The taking of the origin of the times is done when the excitement stops.

In addition, the resolution of the equation system (22) is similar to that performed for the determination of thermal variations during the excitation and following the change of function (19).

The thermal evolution obtained is expressed in the present case:

$$T(x,t') = \frac{2qe}{\lambda} \sum_k \frac{[\cos U_k (\frac{x}{1}) + \frac{p}{U_k \sin U_k (\frac{x}{1})}]}{(U_k^2 + p^2 + 2p)} (1 - e^{-\frac{aU_k^2 t}{e^2}}) (e^{-\frac{aU_k^2 t'}{1^2}})$$

For the case of a brief signal, that is to say, tends to 0, the exponential  $-a U_k^2 t/1^2$  can be approximated by the quantity  $1 - a U_k^2 t/1^2$  and the thermal expression at following the excitement is expressed:

$$T(x,t') = \frac{2qt_0}{\rho c l} \sum_k \frac{[\cos U_k (\frac{x}{1}) + \frac{p}{U_k \sin U_k (\frac{x}{1})}]}{1 + \frac{(p^2 + 2p)}{U_k^2}} (1 - e^{-\frac{aU_k^2 t'}{1^2}}) \tag{23}$$

One of the characteristics of this function makes it possible to write the following equation for two materials which are characterized by:

1.  $a_1$  and  $a_2$ : their diffusivities
2.  $l_1$  and  $l_2$ : their thicknesses
3.  $p_1 = p_2 = p$ : their identical reduced exchange coefficients

$$\frac{a_1 t_{\max 1}}{l_1^2} = \frac{a_2 t_{\max 2}}{l_2^2}, \quad \forall x$$

$t_{\max 1}$  et  $t_{\max 2}$  being the times corresponding to the maximum temperatures. Similarly, for the characteristic times  $(t_{5/6})_1$  et  $(t_{5/6})_2$  corresponding to the 5/6 of the maximum thermal rise, we obtain:

$$\frac{a_1 (t_{5/6})_1}{l_1^2} = \frac{a_2 (t_{5/6})_2}{l_2^2} \tag{24}$$

The expression of the temperature for  $x = 1$  is relative to the practical case of the experimental setup. From relations (23) and (24), the following results can be obtained:

For  $0 \leq t \leq t_0$

$$T(1, t) = \frac{2ql}{\lambda} \sum_k \frac{[(-1)^{k+1}]}{(U_k^2 + p^2 + 2p)} \left(1 - e^{-\frac{aU_k^2 t}{l^2}}\right) \tag{25}$$

For  $t \geq t_0$

$$T(x, t) = \frac{2ql}{\lambda} \sum_k \frac{[(-1)^{k+1}]}{(U_k^2 + p^2 + 2p)} \left(1 - e^{-\frac{aU_k^2 t_0}{l^2}}\right) \left(e^{-\frac{aU_k^2 (t-t_0)}{l^2}}\right) \tag{26}$$

**Results and discussion:-**

**Compressive and tensile strength:-**

Fig. 2. indicates compressive and tensile strength according to binary concretes densities. For density from 1375 Kg/m<sup>3</sup> to 1560Kg/m<sup>3</sup>, this fig shows that strength decreases while density increases. The drop in compressive strength is more important than that of the tensile strength. This phenomenon is due to the fines which have an impact on the microcracking phase. Moreover, a drop in mixing water would allow mitigating partly this drop in resistance and to consequently improve mechanical properties of material, because water dosage links strictly to porosity.

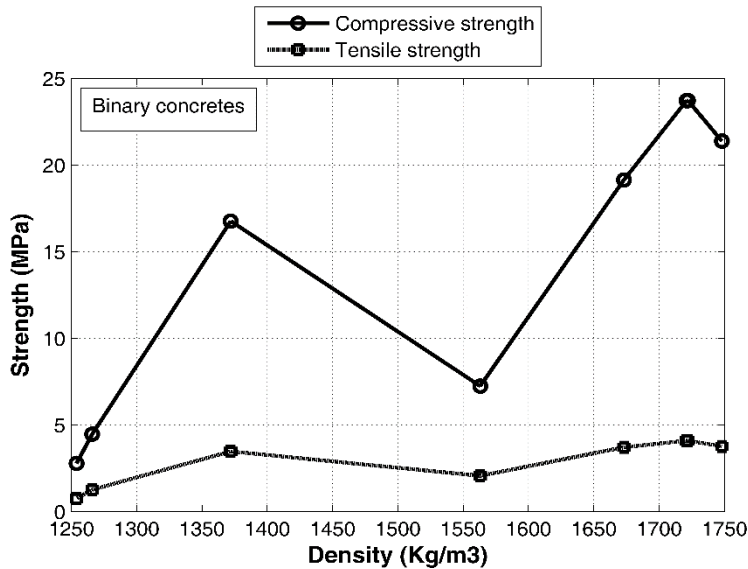


Fig.2. Compressive and tensile strength according to binary concretes densities

Fig. 3:-indicates the variation of the ternary concretes strength for series A according to densities.

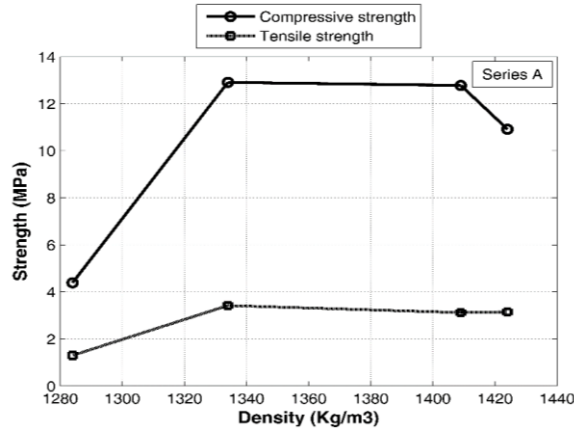


Fig.3. Variation of strength of series A according to densities.

We noticed big results dispersion around the strength average values for the densities from 1408Kg/m<sup>3</sup> to 1425 Kg/m<sup>3</sup>. The higher dispersion, compared with the average value, is 23% for the compressive strength against 1.5% for the tensile strength.

These results were unexpected; the two plots of strength (compressive and tensile) should have the same aspect since samples have nearly equal porosity value. So, we concluded that strengths are modified by a volume scale effect.

Fig. 4:-shows the variation of the ternary concretes strength for series B according to densities.

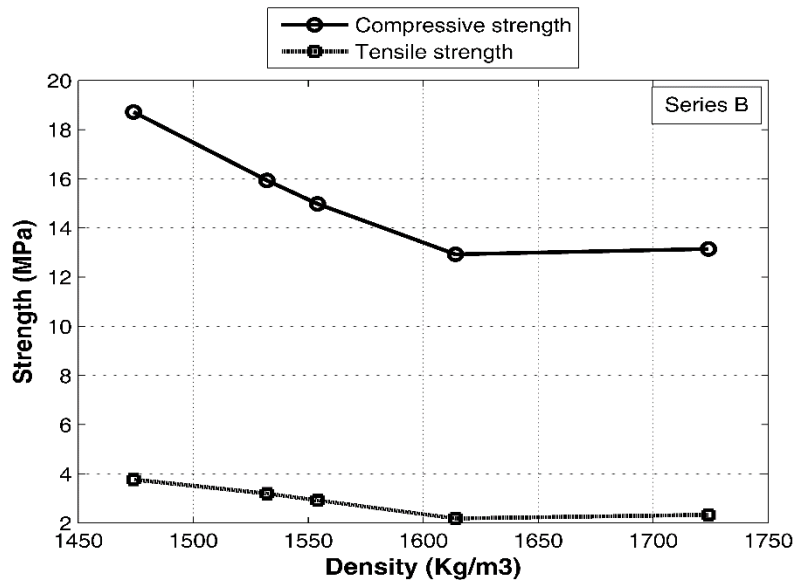


Fig.4:-Variation of strength of series B according to densities.

With big aggregates, porosity is more significant which explains the drop in strength. The drop in compressive strength decreases by 5% when density exceeds 1620 Kg/m<sup>3</sup>.

Fig. 5. shows the variation of the ternary concretes strength for series C according to densities.

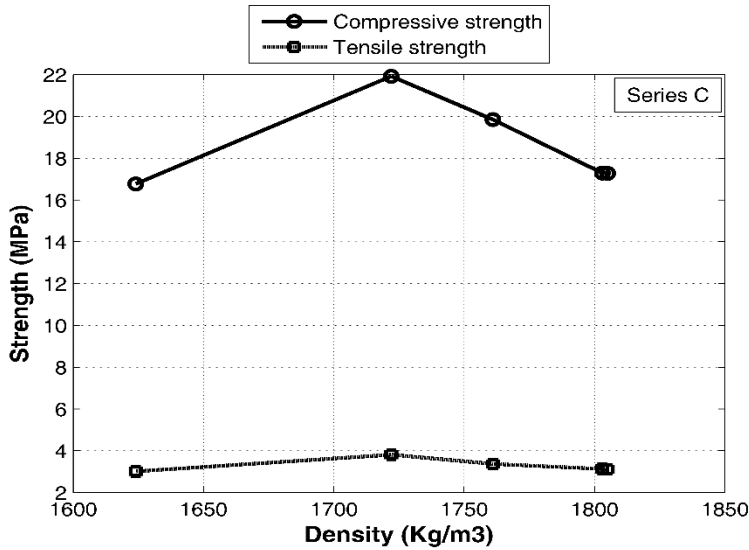


Fig.5.-Variation of strength of series C according to densities.

On this figure, we notice an increase in compressive strength while density is increasing (Compressive strength max =22MPa for density=1720 Kg/m<sup>3</sup>) and then it decreases. The concretes tensile strength is 10 times weaker than the compressive strength.

Compressive strength varies according to the cement dosage (concrete 250 to 450 Kg/m<sup>3</sup>) from 4.39 to 21.92 MPa at 28 d. Fig 5 and 6 show a significant perturbation on strengths. For sure, the cement dosage has an impact on them, but these ones decrease when there is a fine significant amount because of the aggregates specific surface increase. We can also assert that strongest concretes are less porous ones.

Fig. 6.-shows the perturbation caused by the fines on the strength of binary concretes.

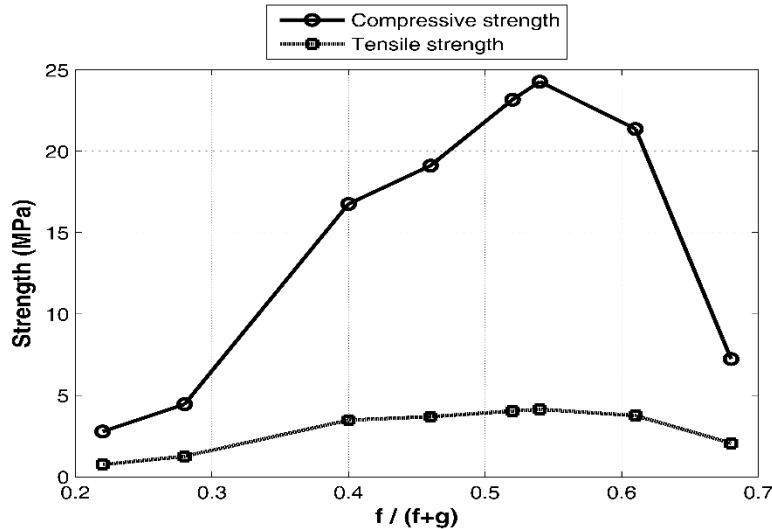


Fig.6.-Perturbation caused by the fines on the strength of binary concretes.

The fine fraction increases from 0.53 to 0.68 triggers strength reduction (compressive and tensile). The granular arrangement smallest packing density is due to the partial reduction of the big aggregates. It increases concrete porosities.

The grain size is also an element which has an impact on lightweight concretes compressive strength which is straighter because the binder-aggregate bonding quality is better and because the aggregate units and bonding

quantities are similar. In fact, the big aggregate fragmentation takes place through the biggest pores which are thus eliminated. We can notice the positive influence on strength in reducing the aggregate maximum sizes (Ganesh Babu and Saradhi Badu's) [35] This phenomenon is also confirmed by Miled K. and co [36] , who worked also on polystyrene concrete, especially on concrete with low aggregates percentage. This phenomenon is not considerable on significant volumetric concentrations.

Fig 7 shows the variation of strength for ternary concretes according to sand and fine content.

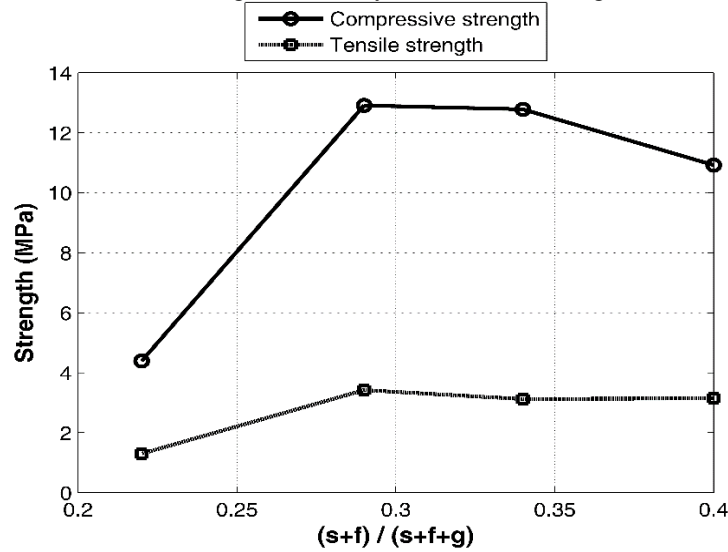


**Fig.7:-**Variation of strength of ternary concretes according to sand and fines content

Usually, only characteristics such as the aggregate porosities are taken into account. However, other characteristics, mentioned in the bibliography, have an impact on concrete properties. These characteristics are: the granulometric distribution, the fine percentages and the material densification. At the beginning, when we put sand, the compressive and tensile strength started to increase. Then, we noticed a progressive dispersion decrease with a ratio formula:  $(s+f)/(s+f+g)$ , between the tensile strength and the compressive strength.

The presence of fine among these aggregates can also influence the relation between their densities and mechanical properties.

Fig. 8. allows to define all different assignments possible on the mass basis and the strength.

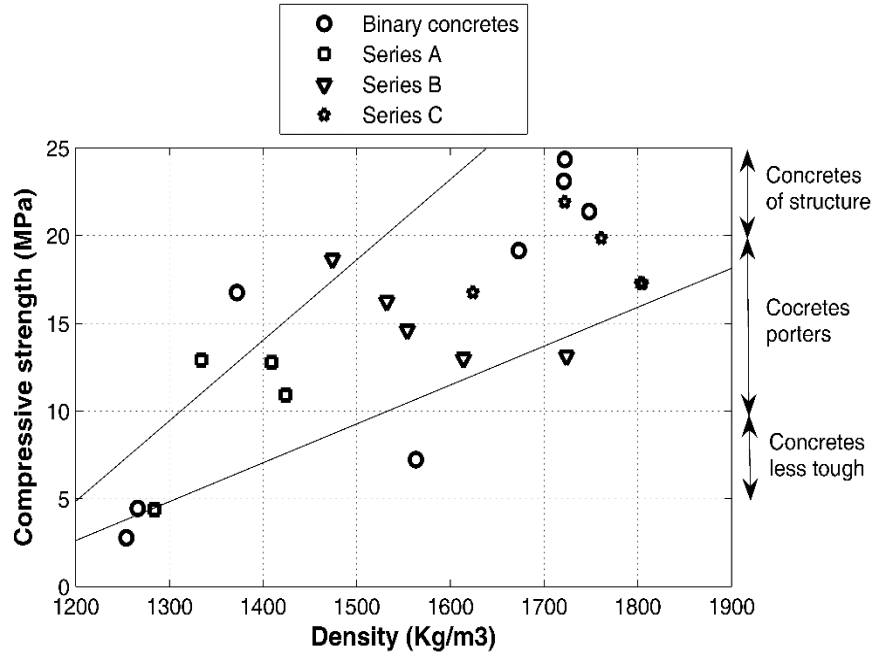


Fig.8:-Compressive strength as a function of densities.

It shows concretes compressive strength as a function of densities. Comparisons between the different series show that the concretes mechanical properties differences are also due to their aggregate percentages and microstructure. Only the concretes density values C3 and C4 are superior to 1800 Kg/m3. They increase, on one side, with the fine introduction for the binary concretes, and on the other side, with the sand and fine introduction for the ternary concretes. The ratio E/C has a significant impact on the hydrated cement paste because it has an influence on the initial space between cement and grains suspended in the mixing water (Chen and co. [37]). The more the water/cement ratio is high, the more the porosity is significant (Baaroghel - Bouny and co [38]). This triggered the strength decrease.

This type of production is applied to almost all types of lightweight concretes and can be used in many fields at a mechanical level. So, according to the classification made by the ACI [39], there are: highly resistant concretes ( $R_c > 20\text{MPa}$ ) that can be used as structural concretes, moderate strength concrete (compressive strength included between 10 and 20 MPa) that can be used for load-bearing elements and low strength concretes that can be used to make beam filling for masonry. Thermal variation impacts on the concretes behavior are to discuss.

**Conductivity and diffusivity:-**

The results of the thermal conductivity measurements are shown in Tables 7 and 8.

Table 7:-Values of the conductivities of concretes without sand in W / mK.

n°	1	2	3	4	5	6	7	8
$\lambda$ [W/mK]	0,403	0,395	0,382	0,310	0,269	0,208	0,332	0,289

Table 8:-Conductivity values of concretes with sand in W / mK

Series	n°	$\lambda$ [W/mK]
A	1	0,258
	2	0,300
	3	0,381
	4	0,386
B	1	0,402
	2	0,453
	3	0,484

	4	0,525
	5	0,545
C	1	0,422
	2	0,566
	3	0,617
	4	0,648
	5	0,658

We have used stationary methods even if this entails a great difficulty of making large compacts. For an appreciable saving of time and an ease of implementation of the sample, we compared the results obtained by the unsteady methods.

It may be noted that the values of the conductivities of concretes without sand are more or less low and less than 0.403 W / mK.

Humidity significantly affects thermal conductivity, as well as other physical parameters. But in this study, our goal is to follow rather the disruption of the concrete structure on the physical parameters.

From the results obtained, we found that the thermal conductivity increases according to the rate of sand. This result is valid throughout the range of variation of the water content of the samples, which can be explained by the fact that the addition of sand brings to the initial material many fine elements that clog the pores created by the proximity large particles. We also found that the thermal conductivity increases with the water content.

Tables 9 and 10 give the values of the thermal diffusivity of concretes.

The values of the diffusivities are between  $2,70 \times 10^{-7}$  m<sup>2</sup>/sand  $5,03 \times 10^{-7}$  m<sup>2</sup>/s.

**Table 9:-** Values of the diffusivity of concretes without sand in  $10^{-6}$  m<sup>2</sup>/s

n°	1	2	3	4	5	6	7	8
$\partial$ [ $10^{-6}$ m <sup>2</sup> /s]	0,427	0,415	0,407	0,358	0,341	0,277	0,402	0,387

**Table 10:-** Values of concrete diffusivities with sand in  $10^{-6}$  m<sup>2</sup>/s

Series	n°	[ $10^{-6}$ m <sup>2</sup> /s]
A	1	0,271
	2	0,371
	3	0,390
	4	0,392
B	1	0,423
	2	0,458
	3	0,506
	4	0,530
	5	0,548
C	1	0,467
	2	0,487
	3	0,528
	4	0,553
	5	0,555

The variations of diffusivities are similar in appearance to those of the conductivities following the introduction of fines and sand. Those heavily dosed in sand are the most diffusive concretes. This situation is normal because of the compactness of these grains.

**Conclusion:-**

1. The analysis of the test results leads to the conclusion that no real workability is encountered in the mixtures when using the pozzolan and superplasticizer up to 1.40% by volume, for purposed slump value. However, Cement-superplasticizer mixtures require more mixing and placing time than that of the control samples.
2. The renewed interest in the pozzolan material is widely justified; it is a local material par excellence. Pozzolan concrete can serve as a carrier insulation in the field of individual constructions.
3. For High Performance Pozzolan Concrete, the compressive strength is significantly improved compared to control concrete
4. At 365 days of preservation, there is a compression strength gain of about 38% and tensile strength of 30%. This result was predictable knowing the beneficial role of using a water reducing superplasticizer.
5. The compositional methods and pozzolan materials available today make it possible to adapt the properties of concrete to the new requirements and make it possible to use it in thermomechanical domains.

**Bibliography:-**

1. Lorenza, C., Stefania, M., & Chiara, B. (2016). Superplasticizer Addition to Carbon Fly Ash Geopolymers Activated at Room Temperature. *Materials*, 9(7): 586. doi: [10.3390/ma9070586].
2. Roshan, T., & Mishara, S.P. (2013). Experimental Studies on Property of Concrete due to Different Ingredient based Super Plasticizer. *International Journal of Science, Engineering and Technology Research*, 2(5), 2278 –7798.
3. Khudhair, M.H., Elharfi, A., & Salahdine, M.E.Y. (2018). The Effect of Polymeric Admixtures of Water Reduce of Superplasticizer and Setting Accelerator on Physical Properties and Mechanical Performance of Mortars and Concretes. *Journal of Environmental Research*, 1(4).
4. Karumanchi, M., Avula, G., Regulagunta, M., & Vipparla, V.B. (2018). Design of high strength concrete-m100 by using silica fume and super plasticizers. *Laetsd journal for advanced research in applied sciences*, 5(7), 394-8442. <http://iaetsdjaras.org/>
5. Erniati, Wihadi, M.T., Zulharnah., & Ulva, R.I. (2015). Porosity, pore size and compressive strength of self compacting concrete using sea water. *Procedia Engineering, Elsevier*, (25) 832-837. doi: 10.1016/j.proeng.2015.11.045.
6. Bu, J., & Tian, Z. (2016). Relationship between pore structure and compressive strength of concrete: Experiments and statistical modeling. *Indian Academy of Sciences, Sadhana 3* (41), pp. 337–344.
7. ASTM C150 (2009). Standard specification for Portland cement. 10 pp. doi:10.1520/C0150\_C0150M-09.
8. ASTM C1602 (2009). Standard Specification for Mixing Water Used in the Production of Hydraulic Cement Concrete.
9. ASTM C 618 (2001). Standard specification for coal fly ash and raw or calcined natural pozzolan for use as a mineral admixture in concrete, ASTM C618-00, Annual Book ASTM Standard 04.02, 310-313.
10. NF EN 934-2 (2009). Admixtures For Concrete Mortar And Grout.
11. Noufid, A., & Belattar, S. (2018). Use of Fillers for Optimal Formulation of Self-Compacting Concretes. *Civil Engineering Journal* 4(1):67, doi: 10.28991/cej-030969.
12. Yousfi, S., Nouri, L., Messaoud, S., & Hadjab, h. (2013). The use of the dreux-gorisse method in the preparation of concrete mixes: An automatic approach. *Asian Journal of Civil Engineering* 15(1):79-94.
13. Nguyen, N.H., anne-lise, B., Ortola, S., & Albert, N. (2013). Influence of the volume fraction and the nature of fine lightweight aggregates on the thermal and mechanical properties of structural concrete. *Construction and Building Materials*, 51:121–132, doi: 10.1016/j.conbuildmat.2013.11.019.
14. Ramachandran, V.S., Beaudoin, J.J., & Shihua, Z. (1989). Control of slump loss in superplasticized concrete. *Materials and Structures* 22(2), doi: 10.1007/BF02472281.
15. ASTM C 33-03 (2003). Standard specifications for concrete aggregates.
16. ASTM C39 / C39M – 18. Standard Test Method for Compressive Strength of Cylindrical Concrete Specimens
17. Bessenouci, M.Z., Triki, N.E.B., Khelladi, S., Draoui, B., & Abene, A. (2011). The apparent thermal conductivity of pozzolana concrete. *Seventh International Conference on Material Sciences (CSM7), Beirut–Lebanon. Elsevier-Physics Procedia* 21, 59–66